Spatial Wilson Loops in Holographic QCD Models and Experimental Observables

Pavel Slepov

Based on paper I.Y. Aref'eva, A.Hajilou, K.Rannu and P.Slepov, Phys. Rev. D **113** (2026) no. 106004 [arXiv:2601.09611 [hep-th]].

Steklov Mathematical Institute of Russian Academy of Sciences

QUARKS-2026,
Petrozavodsk, Russia

18.05.2026

Studies of QCD Phase Diagram is the main goal of new facilities

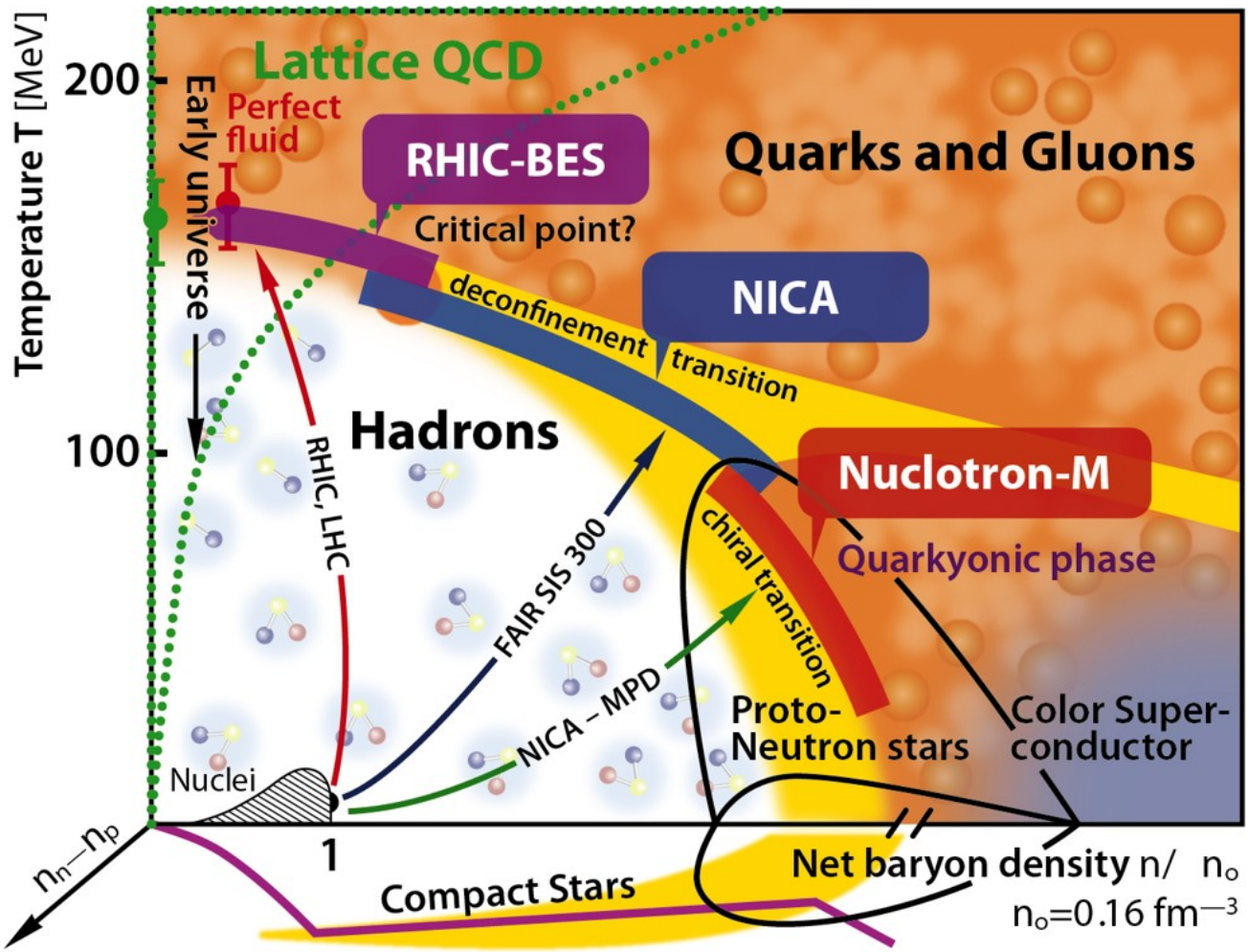

From: https://nica.jinr.ru/physics.php

Holographic QCD phase diagram for light quarks

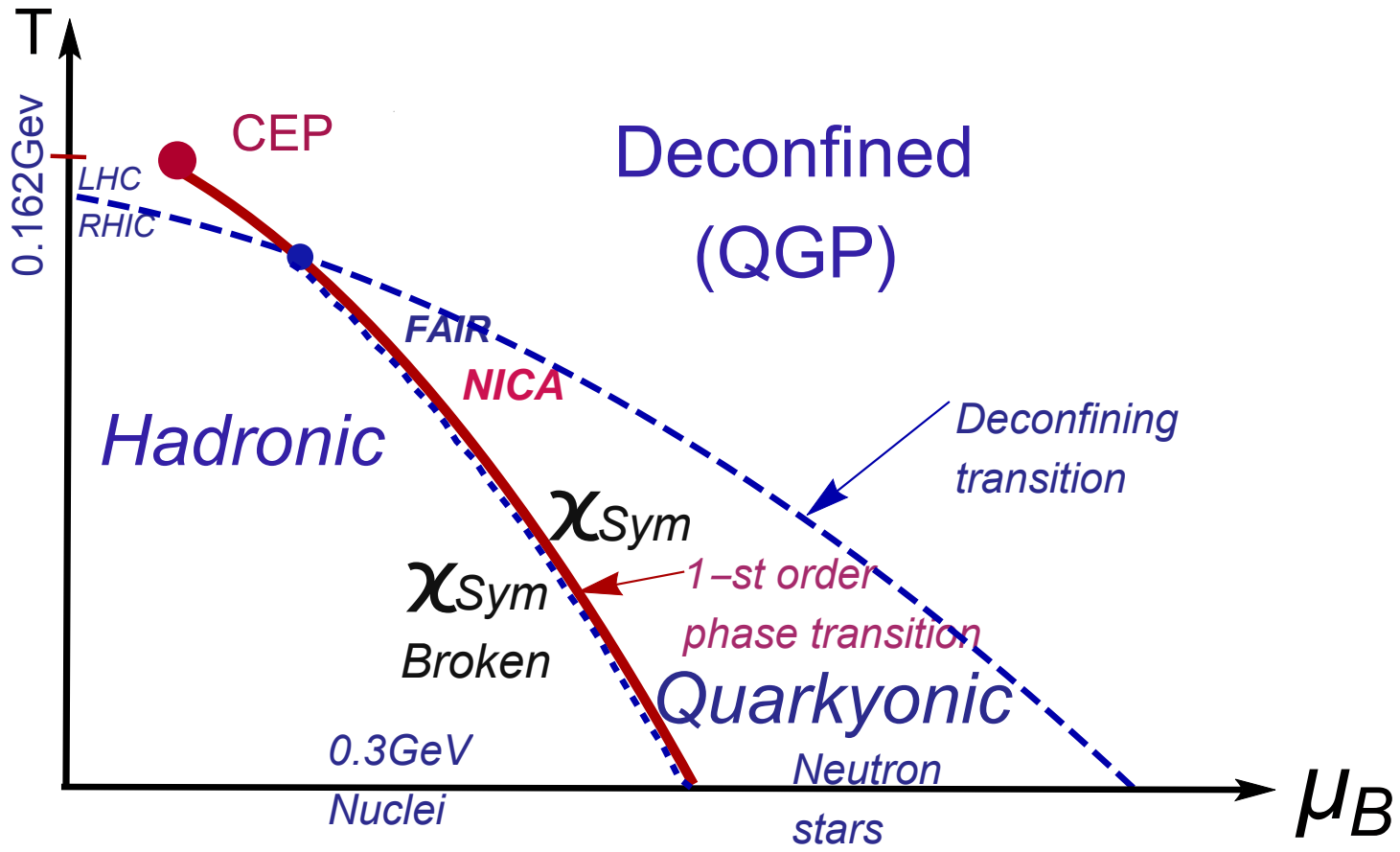

Motivation

Purpose: Study of the QCD phase diagram in (μ,T) plane for the fully anisotropic background

Multiplicity $\mathcal{M} \propto s_{AdS}^{0.33}$ vs $\mathcal{M} \propto s_{LHC}^{0.155}$

$\mathcal{M} \propto s^{\frac{1}{\nu+2}}$, $\nu = 4.5$ I.Aref'eva, A.Golubtsova, JHEP **04**, 011 (2015)

Strong magnetic field at the early stages of HIC: $eB \sim 0.3 GeV^2$

QCD Phase Diagram: Lattice

Phase diagram
on quark mass

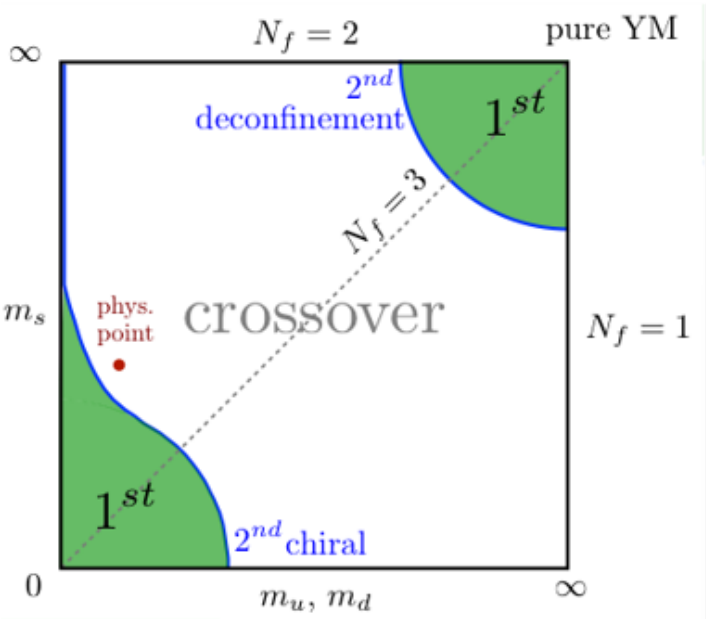

Columbia plot
Brown et al., PRL (1990)

Main problem with $\mu \neq 0$
Imaginary chemical potential method

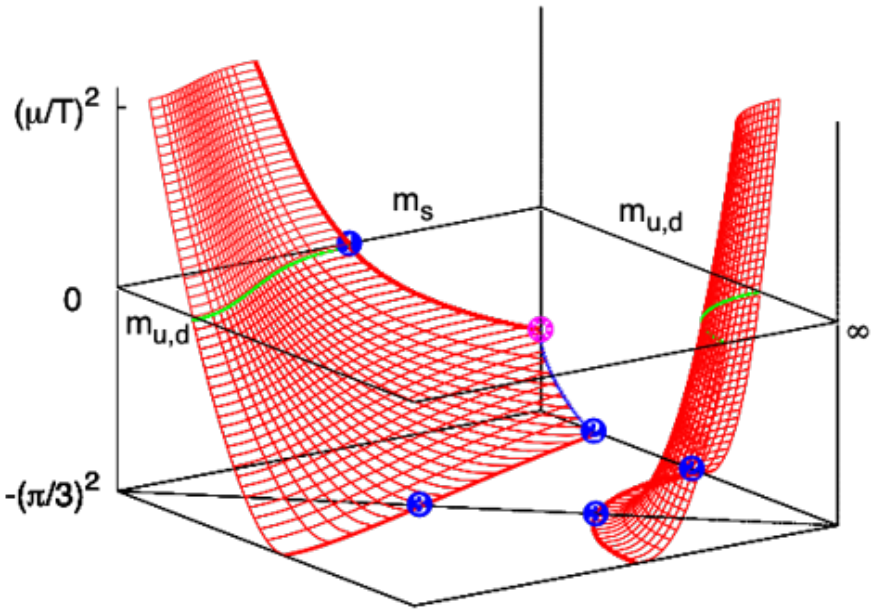

Philipsen, Pinke, PRD (2016)

"Light" and "Heavy" Quarks from Columbia Plot

Light quarks

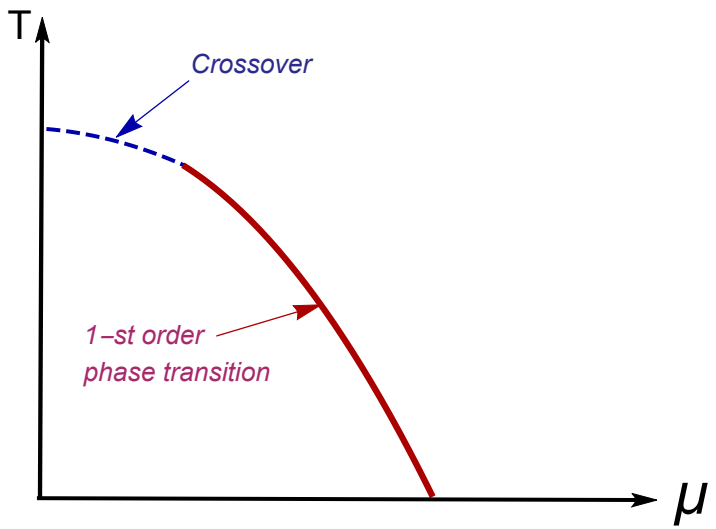

Heavy quarks

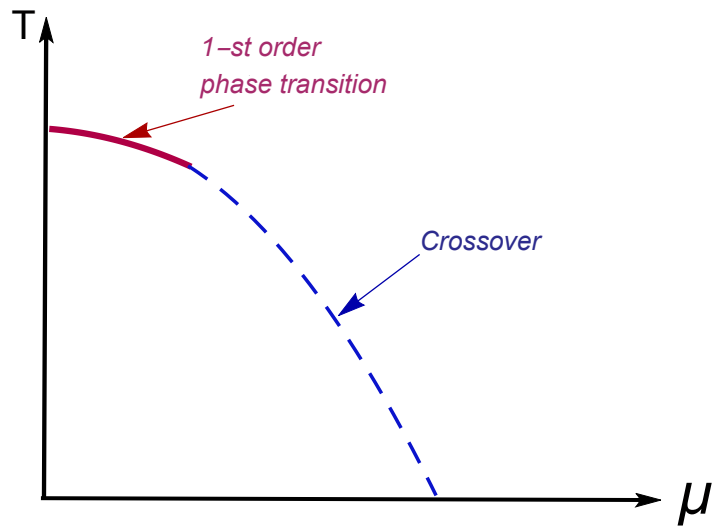

Temperature as function of horizon for different μ in isotropic models for light and heavy quarks

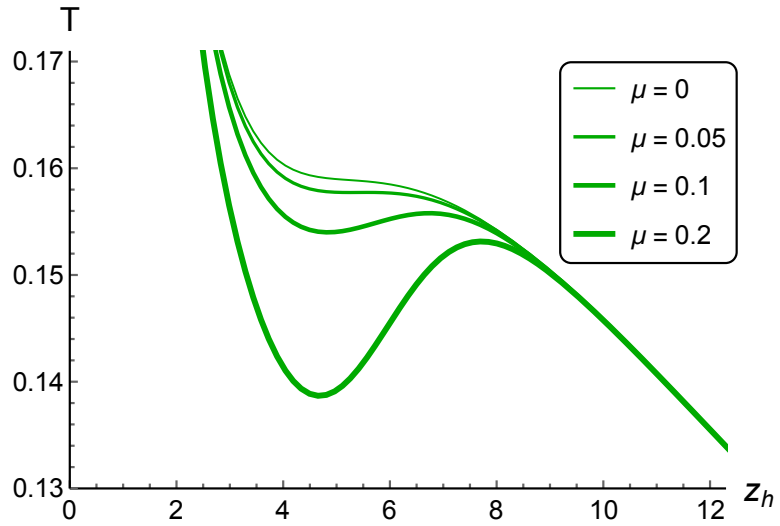

Light Quarks $b(z) = e^{-2\,a\,\ln(bz^2+1)}$

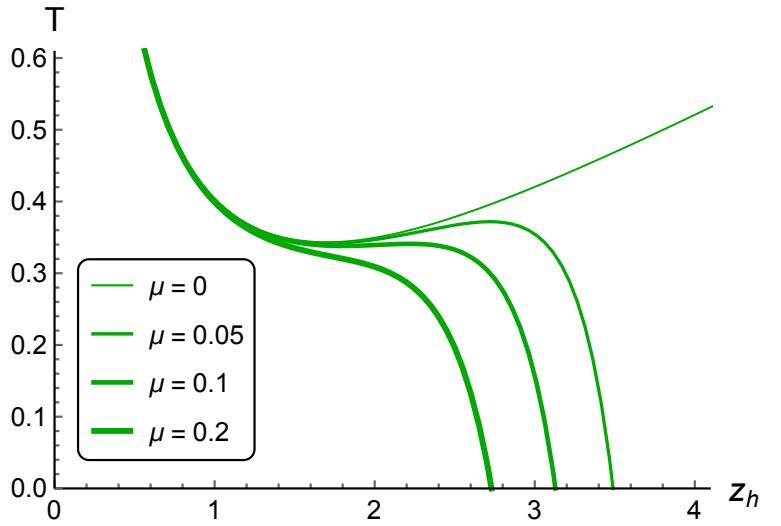

Heavy Quarks $b(z) = e^{-cz^2/4}$

The main question to discuss is: what directly measurable quantities indicate the 1st order phase transition?

- Jet Quenching – I. Y. Aref'eva, A. Hajilou, A. Nikolaev and P. S., "Jet quenching in holographic QCD as an indicator of phase transitions in anisotropic regimes," PRD **112** (2025) 126007
- Energy loss – I. Y. Aref'eva, A. Hajilou, K. Rannu and P. S., "Spatial Wilson Loops and Energy Loss for Heavy Quarks...," PRD **113** (2026) 106004
- Direct photons – I.Ya. Aref'eva, A. Ermakov and P. S., "Direct photons emission rate ... with first-order phase transition," EPJC **82** (2022) 85
- Cross-sections – I.Ya.Aref'eva, A. Hajilou, P. S. and M. Usova, "Running coupling for HQCD...: Isotropic case," PRD **110** (2024) 126009
  I.Ya. Aref'eva, A. Hajilou, A. Nikolaev and P. S., "HQCD running coupling ... in strong magnetic field," PRD **110** (2024) 086021

Holographic model of an anisotropic plasma in a magnetic field at a non-zero chemical potential

I.Aref'eva, K.Rannu'18; I Aref'eva, K. Rannu, P.S.'21

$$S=\int d^5x\,\sqrt{-g}\left[R-\frac{f_1(\phi)}{4}F^2_{(1)}-\frac{f_2(\phi)}{4}F^2_{(2)}-\frac{f_B(\phi)}{4}F^2_{(B)}-\frac{1}{2}\partial_M\phi\partial^M\phi-V(\phi)\right]$$

$$ds^2=\frac{L^2}{z^2}\mathfrak{b}(z)\left[-g(z)\,dt^2+dx^2+\left(\frac{z}{L}\right)^{2-\frac{2}{\nu}}dy_1^2+e^{c_B z^2}\left(\frac{z}{L}\right)^{2-\frac{2}{\nu}}dy_2^2+\frac{dz^2}{g(z)}\right]$$

$$A_{(1)\mu}=A_t(z)\delta^0_\mu \qquad A_t(0)=\mu \qquad F_{(2)}=q_2\,dy^1\wedge dy^2 \qquad F_{(B)}=q_B\,dx\wedge dy^1$$

Giataganas'13; Aref'eva, Golubtsova'14; Gürsoy, Järvinen '19; Dudal et al.'19

$\mathfrak{b}(z)=e^{2\mathcal{A}(z)}$ $\Leftrightarrow$ quarks mass

"Bottom-up approach"

Heavy quarks (c, b):

$\mathcal{A}(z)=-\,cz^2/4$ — *Andreev, Zakharov'06*

$\mathcal{A}(z)=-\,cz^2/4-(p-c_B\,q_3)z^4$ — *Aref'eva, Hajilou, Rannu, P.S.' 23*

Light quarks (u, d, s)

$\mathcal{A}(z)=-\,a\ln(bz^2+1)$ — *Li, Yang, Yuan'17*

$\mathcal{A}(z)=-\,d\ln((az^2+1)(bz^4+1))$ — *Zhu, Chen, Zhou, Zhang, Huang'25*

Boundary conditions

$$A_t(0) = \mu, \quad A_t(z_h) = 0,$$
$$g(0) = 1, \quad g(z_h) = 0,$$
$$\phi(z_0) = 0.$$

Boundary condition for dilaton field

Holographic running coupling $\alpha(z) = e^{\varphi(z)}$

$\varphi(z)$ - dilaton field $\varphi(z)$ is defined up to a constant: $\varphi(z)\Big|_{z=z_0} = 0.$

There are 3 choices: a) $z_0 = 0$ b) $z_0 = f(z_h)$ c) $z_0 = z_h$

Light Quark Model: $z_0 = 10\exp(-z_h/4) + 0.1$

I Aref'eva, K.Rannu, P.S., JHEP'21

With this boundary condition the temperature dependence of σ_s fits the known lattice data

Cordaso, Bicudo 1111.1317

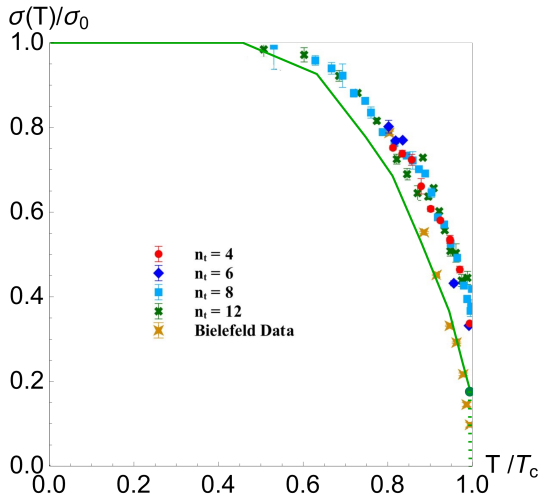

Heavy Quark Model: $z_0 = \exp(-z_h/4) + 0.1$

I.Ya.Aref'eva, A. Hajilou, P. S. and M. Usova, PRD'24

1-st order phase transition for "light" and "heavy" quarks in Holography

Light quarks

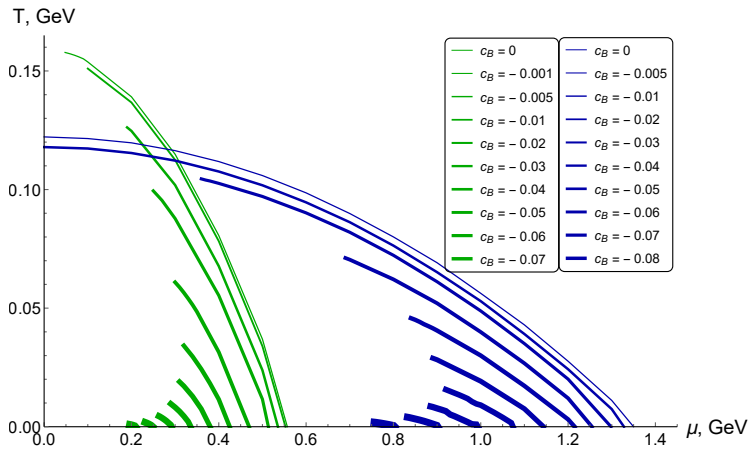

Aref'eva, Ermakov, Rannu, P.S.,EPJC'23

Heavy quarks

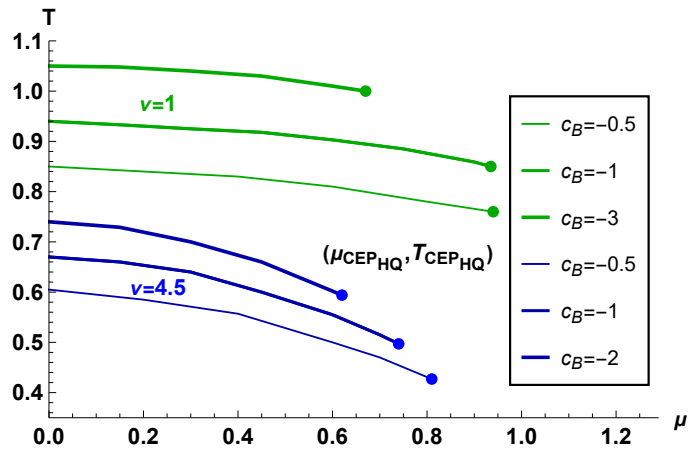

Aref'eva, Hajilou, Rannu, P.S.,EPJC'23

1-st order phase transition for "light" and "heavy" quarks in Holography

Light quarks

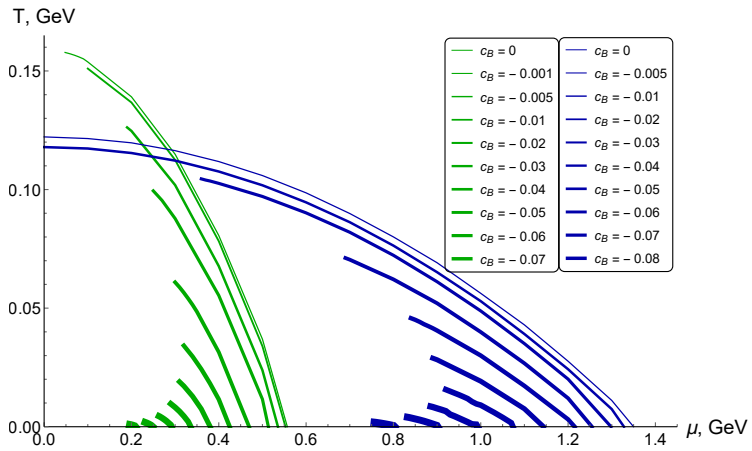

Aref'eva, Ermakov, Rannu, P.S.,EPJC'23

Heavy quarks

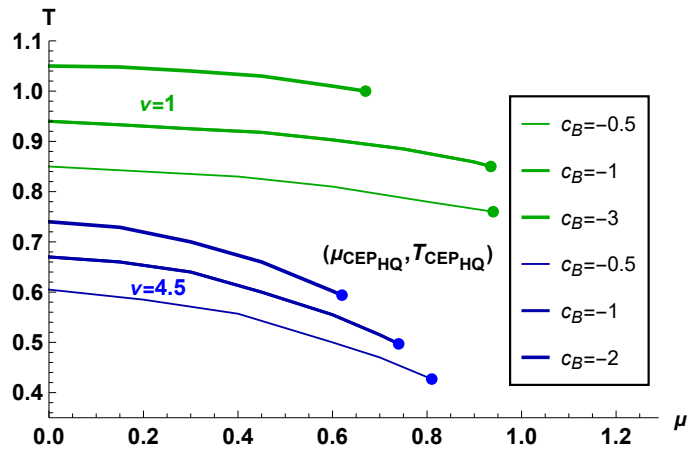

Aref'eva, Hajilou, Rannu, P.S.,EPJC'23

- QCD Phase Diagram from Lattice Columbia plot
  Brown et al.'90 Philipsen, Pinke'16
- **Main problem on Lattice:** $\mu \neq 0$

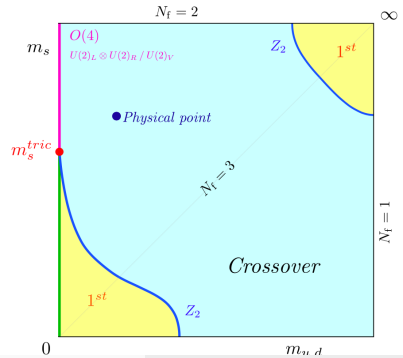

3 types of Wilson loops in quantum gauge theories!

- **Time-like loop** $\mathcal{C} = t \times x, \quad t, x >> \ell_{QCD}$
  $\ell_{QCD} \sim \frac{\hbar c}{\Lambda} \approx 1\text{fm}, W_F[C] \underset{\substack{t\to\infty \\ x\to\infty}}{\sim} e^{-\sigma_{st} t x}$
- **Space-like loop** $\mathcal{C} = x_1 \times x_2, \quad x_i >> \ell_{QCD}$

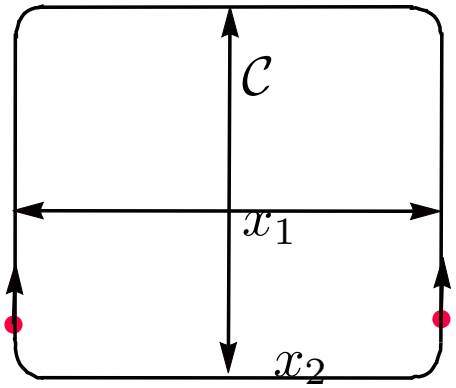

$$W_F[C] \underset{\substack{x_1\to\infty \\ x_2\to\infty}}{\sim} e^{-\sigma_{DF} x_1 x_2}$$

σ_{DF} **drag force parameter**, related with energy loss

- **Light-like loop** $\mathcal{C} = x_- \times x_2, \quad x_- >> x_2$

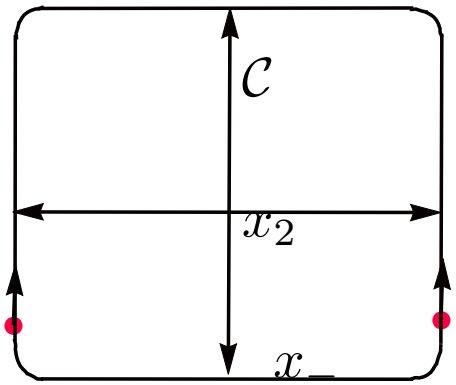

$$W_{Ad}[C] \underset{\substack{x_-\to\infty \\ x_2\to 0}}{\sim} e^{-q\, x_- x_2^2}$$

q - jet quenching parameter

the average transverse momentum squared transferred from the parton to the medium per unit path length

3 types of Wilson loops in quantum gauge theories!

- **Time-like loop** $\mathcal{C} = t \times x, \quad t, x >> \ell_{QCD}$
  $\ell_{QCD} \sim \frac{\hbar c}{\Lambda} \approx 1\text{fm}, W_F[C] \underset{\substack{t\to\infty \\ x\to\infty}}{\sim} e^{-\sigma_{st} t x}$

- **Space-like loop** $\mathcal{C} = x_1 \times x_2, \quad x_i >> \ell_{QCD}$

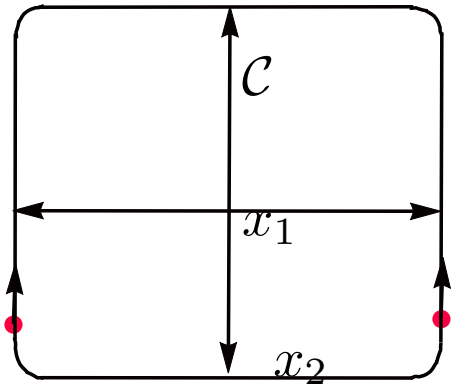

$$W_F[C] \underset{\substack{x_1\to\infty \\ x_2\to\infty}}{\sim} e^{-\sigma_{DF} x_1 x_2}$$

σ_{DF} **drag force parameter**, related with energy loss

- **Light-like loop** $\mathcal{C} = x_- \times x_2, \quad x_- >> x_2$

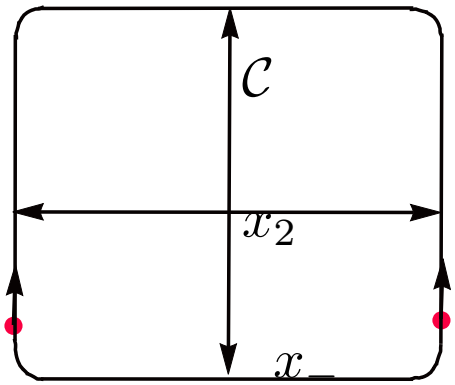

$$W_{Ad}[C] \underset{\substack{x_-\to\infty \\ x_2\to 0}}{\sim} e^{-q\, x_- x_2^2}$$

q **- jet quenching parameter**

the average transverse momentum squared transferred from the parton to the medium per unit path length

- Wilson Loops in holographic QCD **J. Maldacena'98**

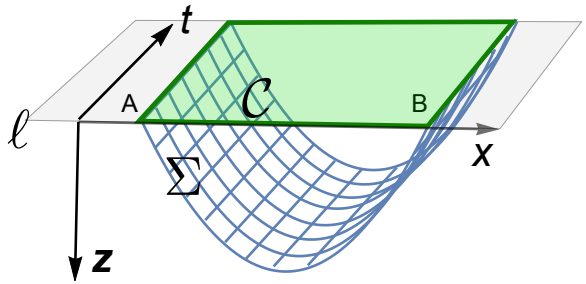

- String action "on a barn"

$$S_{NG} = \int d\tau d\xi\, M(z(\xi)) \sqrt{\mathcal{F}(z(\xi)) + (z'(\xi))^2}$$

H.Liu, K.Rajagopal, U.Wiedemann'06 Conf. case: $q \sim T^3$

Jet quenching for non-zero magnetic field and initial anisotropy. Analytical formula & Numerical results

$$q_i(z_h,\mu,c_B,\nu)=\frac{L^2}{\pi\alpha' a_i}\sim\frac{1}{a_i},\quad i=2,3$$

$$a_2=\int_0^{z_h}\frac{e^{-2\mathcal{A}_s(z)}\left(\frac{z}{L}\right)^{2/\nu}}{\sqrt{g(z)(1-g(z))}}dz\qquad a_3=\int_0^{z_h}\frac{e^{-2\mathcal{A}_s(z)-c_B z^2}\left(\frac{z}{L}\right)^{2/\nu}}{\sqrt{g(z)(1-g(z))}}dz$$

$$g(z,z_h,\mu,c_B,\nu)=e^{c_B z^2}\left[1-\frac{I_1(z)}{I_1(z_h)}+\frac{\mu^2\left(2c-c_B\right)I_2(z)}{L^2\left(1-e^{(2c-c_B)z_h^2/2}\right)^2}\left(1-\frac{I_1(z)I_2(z_h)}{I_1(z_h)I_2(z)}\right)\right]$$

$$I_1(z)=\int_0^z\left(1+b\chi^2\right)^{3a}\frac{\chi^{1+\frac{2}{\nu}}}{e^{\frac{3}{2}c_B\chi^2}}d\chi,\qquad I_2(z)=\int_0^z\left(1+b\chi^2\right)^{3a}\frac{\chi^{1+\frac{2}{\nu}}}{e^{(-c+2c_B)\chi^2}}\,d\chi$$

$$T=\frac{|g'|}{4\pi}\Big|_{z=z_h}\qquad s=\left(\frac{L}{z_h}\right)^{1+\frac{2}{\nu}}\frac{e^{c_B z_h^2/2}\left(1+bz_h^2\right)^{-3a}}{4}\qquad F=\int_{z_h}^{z_{h_2}}s\,dT=\int_{z_h}^{z_{h_2}}s\,T'dz$$

Jet quenching for $c_B = -0.05$ and $\nu = 1$ for LQ model. Numerical results for a_2 and a_3

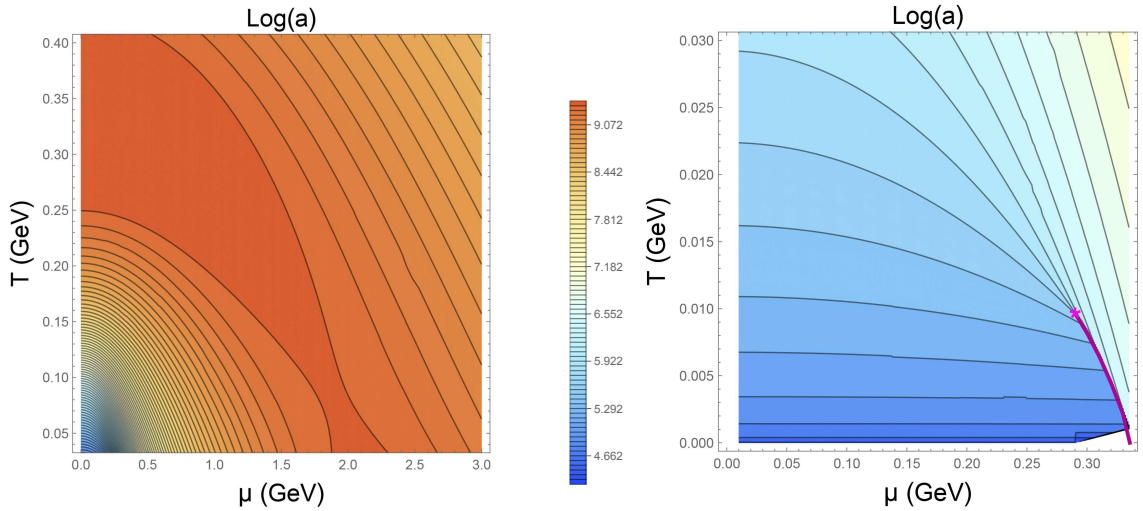

a_2 orientation

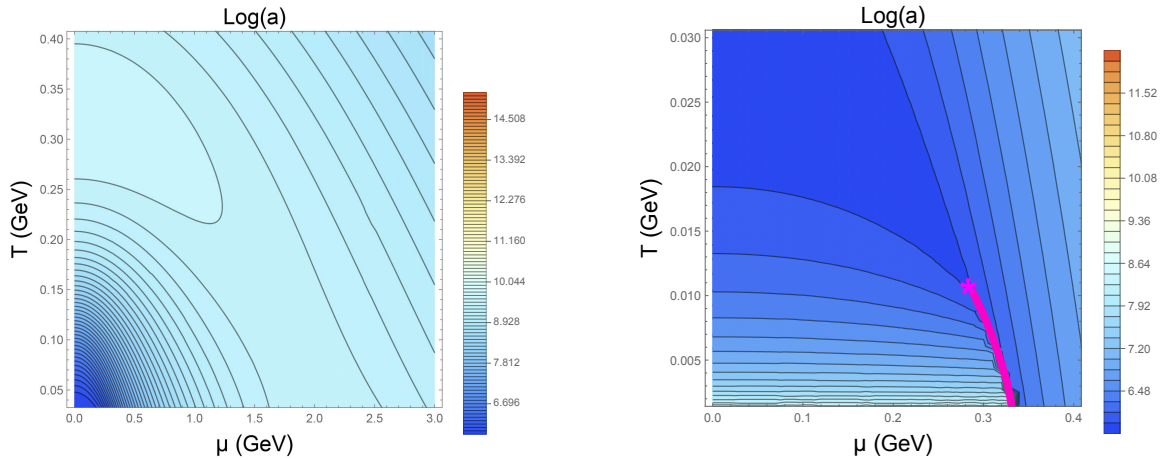

a_3 orientation

String tension for SWLs vs drag forces

String tension σ can be calculated on $z = z_h$ or $z = z_{DW}$ (if the DW exists). The connection between drag forces and string tensions for metric with $\mathfrak{g}_1 = 1$:

$$\sigma_{xY_1}\Big|_{z=z_h} = \frac{\sqrt{\lambda}}{2\pi}\frac{p_x}{v} = \frac{\sqrt{\lambda}}{2\pi}\left(\frac{\mathfrak{b}_s(z_h)}{z_h^2}\right)\sqrt{\mathfrak{g}_2},$$

$$\sigma_{xY_2}\Big|_{z=z_h} = \frac{\sqrt{\lambda}}{2\pi}\frac{p_{y_1}}{v} = \frac{\sqrt{\lambda}}{2\pi}\left(\frac{\mathfrak{b}_s(z_h)}{z_h^2}\right)\sqrt{\mathfrak{g}_3},$$

$$\sigma_{y_1Y_2}\Big|_{z=z_h} = \frac{\sqrt{\lambda}}{2\pi}\frac{p_{y_2}}{v} = \frac{\sqrt{\lambda}}{2\pi}\left(\frac{\mathfrak{b}_s(z_h)}{z_h^2}\right)\sqrt{\mathfrak{g}_2\mathfrak{g}_3}$$

I. Aref'eva Phys.Part.Nucl. **51** 4, 489-496 (2020),
O. Andreev, Mod. Phys. Lett. A **33**, 06 (2018),
S. J. Sin and I. Zahed, Phys.Lett. B **648**, 318 (2007).

Phase transitions of $\mathcal{V}_1$ for $\nu = 1,\ 4.5$ in magnetic catalysis model with modified warp-factor

Modified Warp-factor: $\mathcal{A}(z) = -cz^2/4 - (p - c_B\, q_3)z^4$

Aref'eva, Hajilou, Rannu and P. S., Eur. Phys. J. C 83, 12, 1143 (2023)

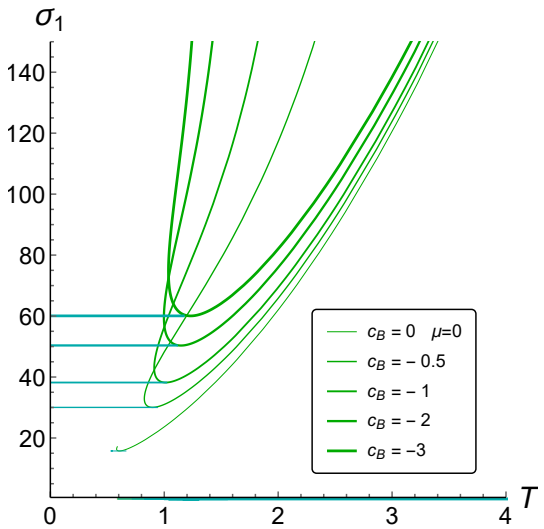

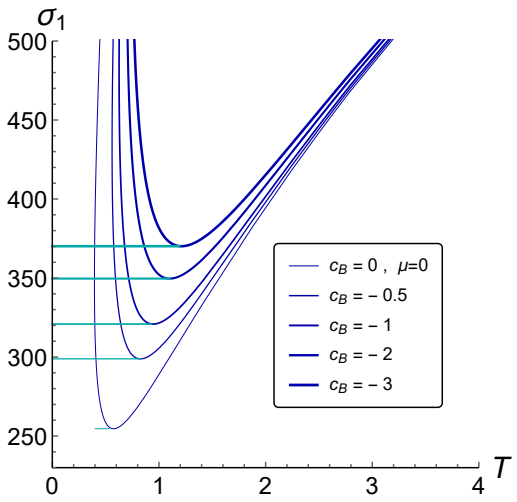

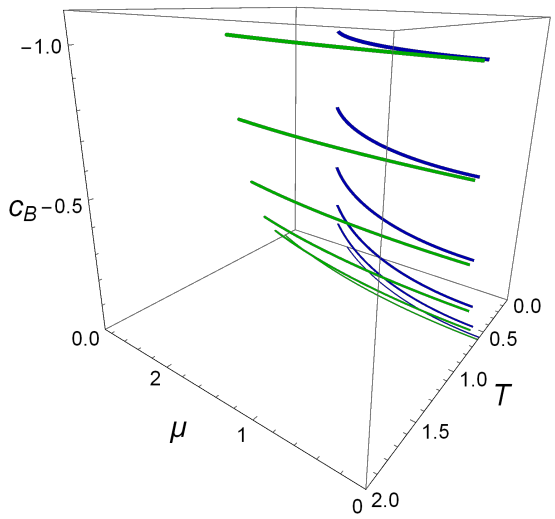

Phase diagrams for SWL in (μ, T)-plane

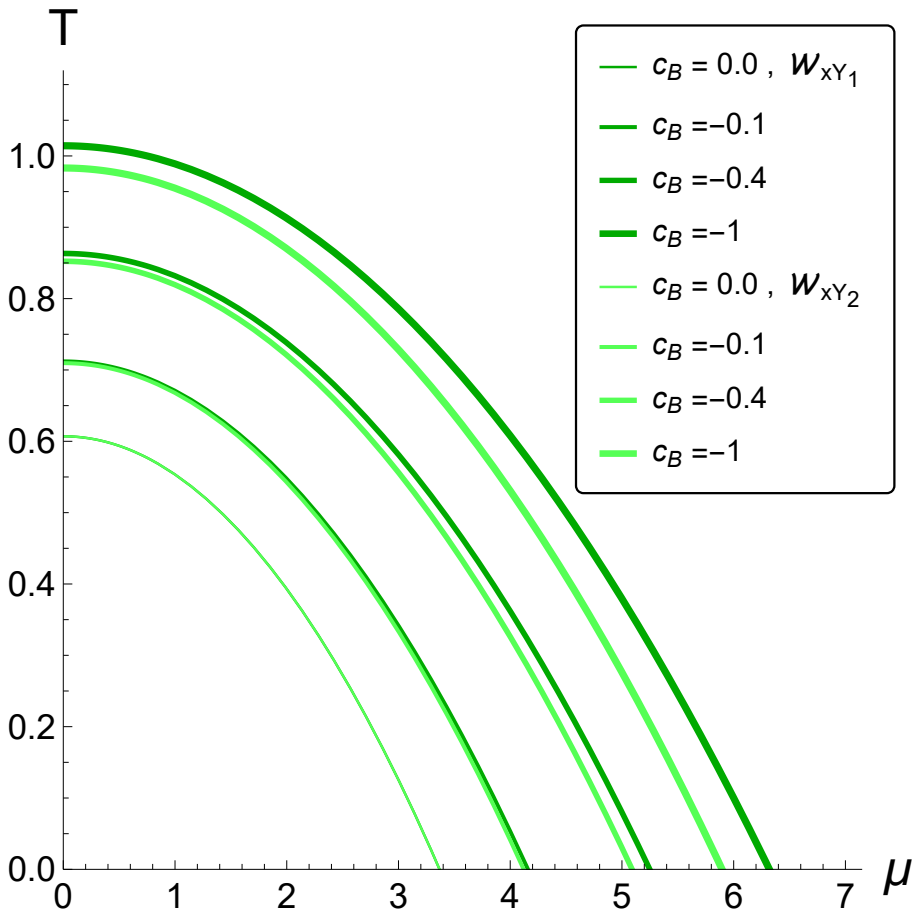

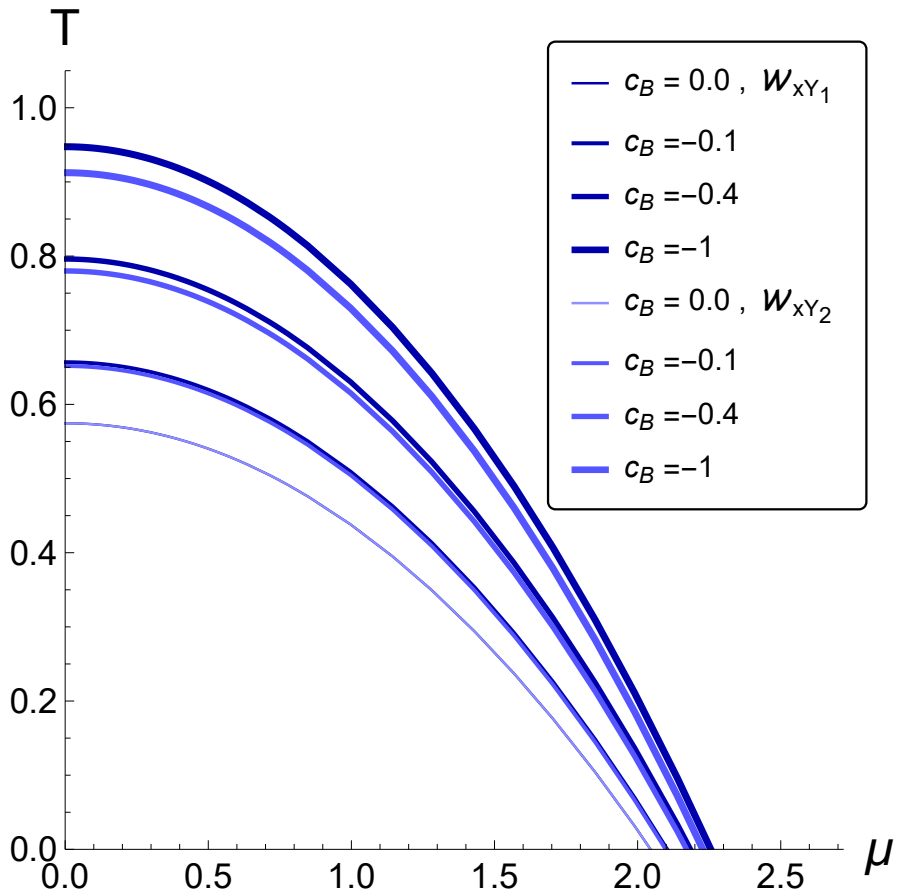

Spatial string tension σ_2 dependence on temperature

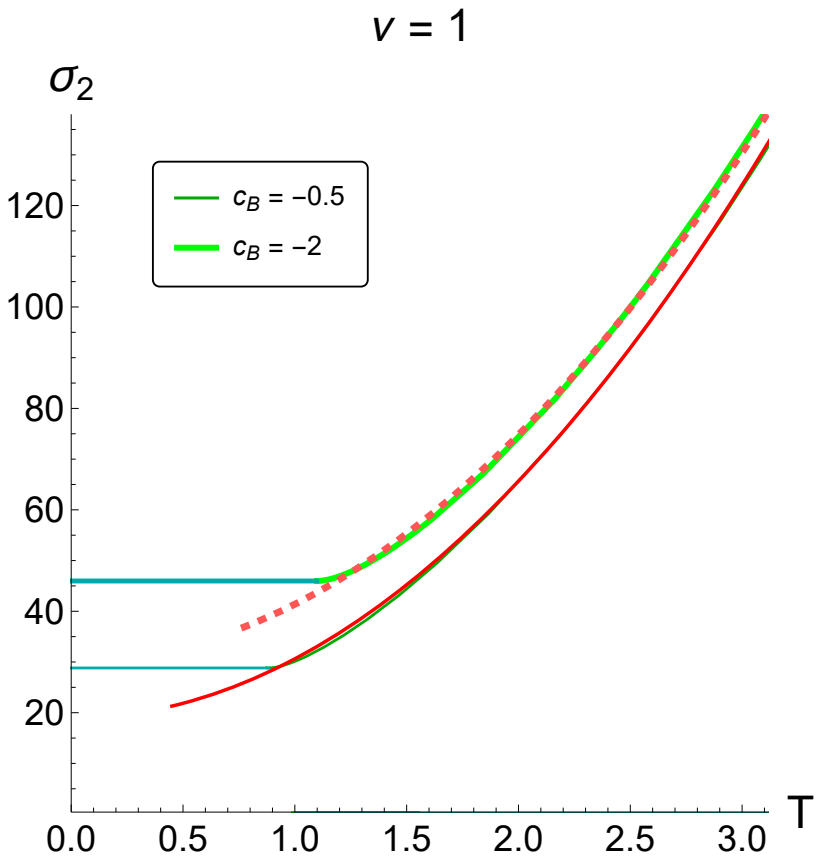

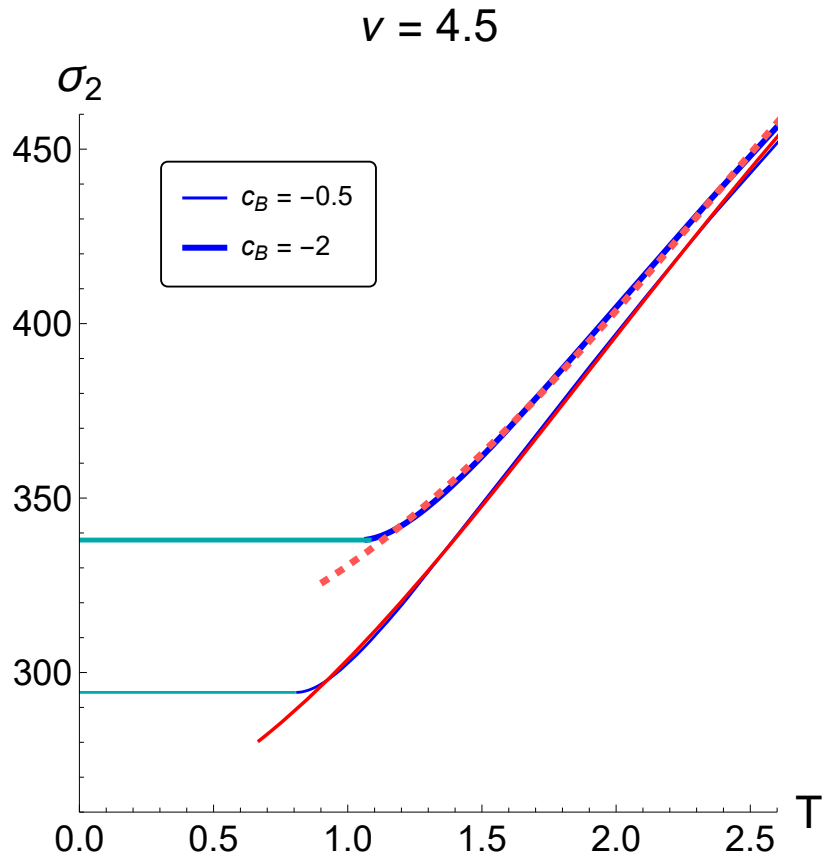

Lattice QCD: $\sigma \sim T^2$
$\sigma_{solid\ red} = 18.9 + 11.7\,T^2$,
$\sigma_{dashed\ red} = 30.2 + 11.1\,T^2$

Non quadratic behaviour of σ in anisotropic case

Experimental observables and drag forces

The nuclear modification factor, specifies the modification of the production yield in nucleus–nucleus collisions relative to pp collisions due to hard partonic scattering processes

$$R_{AA}(p_T) = \frac{1}{\langle N_{\rm coll}\rangle} \cdot \frac{dN_{AA}/dp_T}{dN_{pp}/dp_T},$$

The elliptic flow v_2 which is a measure of the anisotropy in the azimuthal distribution of particle production:

$$\frac{dN}{d\phi} \propto 1 + 2\sum_{n=1}^{\infty} v_i \cos\big(i(\phi - \Psi_i)\big),$$

where ϕ is the azimuthal angle of a particle, Ψ_i is the orientation of the i-th harmonic symmetry plane, and v_2 corresponds to $i = 2$. A positive v_2 indicates a preference for emission in the plane perpendicular to the beam direction (the reaction plane), reflecting the almond-shaped overlap region in non-central collisions.

Experimental observables and drag forces

$$R_{AA}(p_T,\phi) \approx \left(1-\frac{C\,\eta(\phi)\tilde{L}}{p_T}\right)^{n-2} + \frac{n(n+1)}{2}\,\frac{\tilde{L}}{p_T^2}\,\kappa(\phi),$$

$$\begin{aligned}\eta(\phi) &= \eta_{\parallel}\cos^2\phi + \eta_{\perp}\sin^2\phi,\\ \kappa(\phi) &= \kappa_{\parallel}\cos^2\phi + \kappa_{\perp}\sin^2\phi.\end{aligned}$$

The first term represents suppression due to anisotropic drag force, and the second term represents momentum broadening from anisotropic diffusion. Here ϕ is the angle in the transverse plane (the plane perpendicular to the beam axis) between $\vec{p}_T$ and the impact vector. The elliptic flow v_2, is also related to the drag force and momentum broadening

$$v_2(p_T) \simeq -\frac{(n-2)C\tilde{L}}{4p_T}\left(\eta_{\parallel}-\eta_{\perp}\right) + \frac{n(n+1)\tilde{L}}{8p_T^2}\left(\kappa_{\parallel}-\kappa_{\perp}\right).$$

The Einstein relations

$$\eta_{\parallel} = \frac{p_{y_1}}{v} = \frac{\kappa_{\parallel}}{2ET}, \quad \eta_{\perp} = \frac{p_{y_2}}{v} = \frac{\kappa_{\perp}}{2ET}.$$

M. Gyulassy, P. Levai and I. Vitev, PRL **85** (2000), 5535-5538
Y. L. Dokshitzer, D. E. Kharzeev, PLB **519** (2001) 199-206
I. Vitev, PLB **639** (2006), 38-45

$c_B = 0$ $c_B = -0.005GeV^2$ $c_B = -0.05GeV^2$ $c_B = -0.5GeV^2$

$\nu = 1$

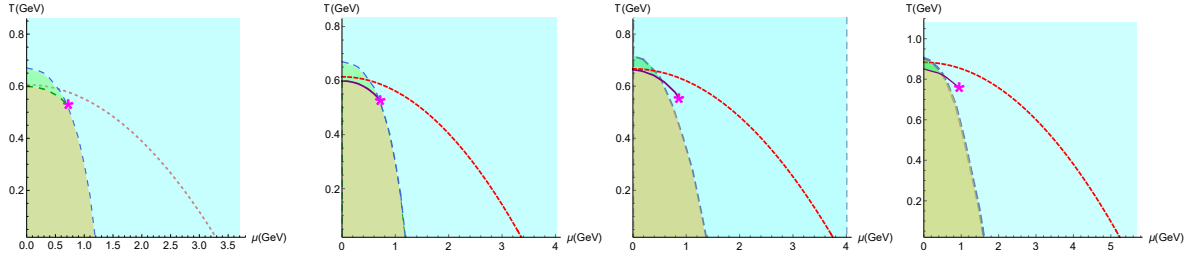

$\nu = 1.5$

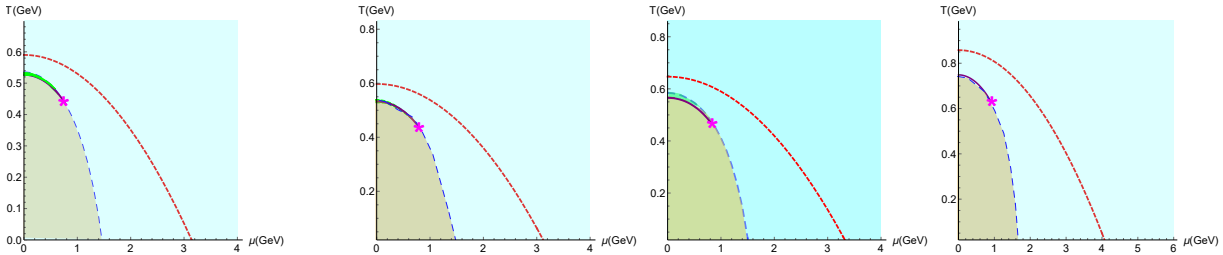

$\nu = 3$

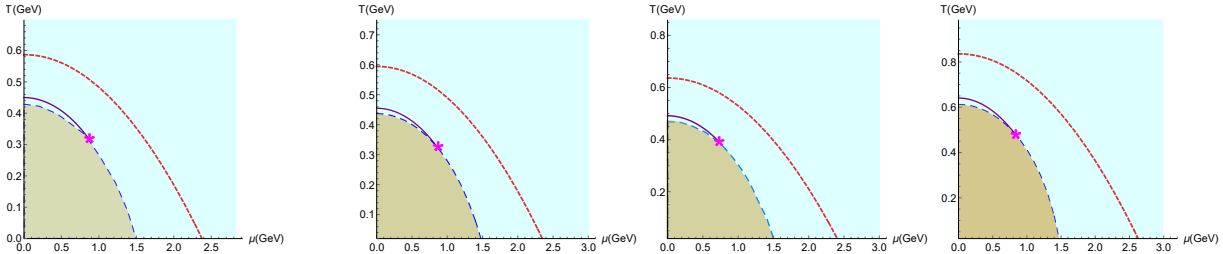

$\nu = 4.5$

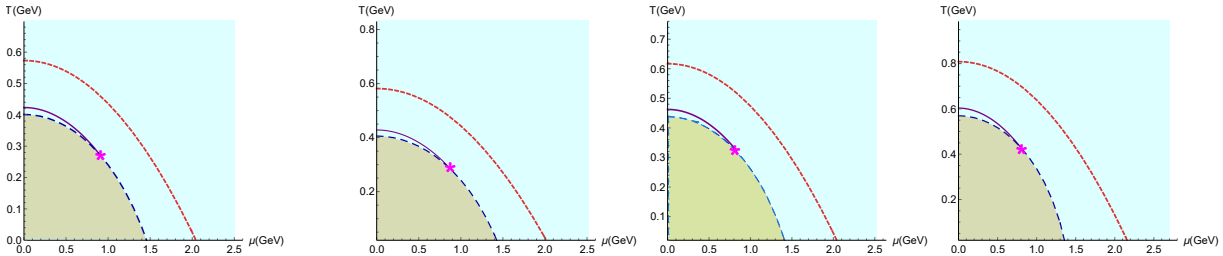

I. Y. Aref'eva, A. Hajilou, K. Rannu and P. S., Phys. Rev. D 113 (2026) no. 106004

Machine Learning in Holographic QCD: Recent Studies

Motivation

Holographic QCD models contain bulk fields and potentials with many free parameters. Machine learning (ML) offers systematic, data-driven ways to fix these parameters and extract physical observables.

	Focus
K. Hashimoto, et al., PRD **98** (2018) 046019	Learning bulk metric from boundary correlators using deep neural network
Y. K. Yan, et al., PRD **102** (2020) 101902	Deep learning black hole metrics from shear viscosity
C. Park, et al., PRD **106** (2022) 106017	Dual geometry of entanglement entropy via deep learning
X. Chen and M. Huang, JHEP **02** (2025), 123	QCD phase diagram in EMD model & CEP with N_f flavors via deep learning

Framework: EMD Model + Machine Learning

Einstein-Maxwell-Dilaton (EMD) Holographic Model

A 5D bottom-up holographic model with action (Einstein frame):

$$S_b = \frac{1}{16\pi G_5}\int d^5x\,\sqrt{-g}\left[R - \frac{f(\phi)}{4}F^2 - \frac{1}{2}\partial_\mu\phi\,\partial^\mu\phi - V(\phi) + ...\right]$$

Analytical solutions are obtained via the **potential reconstruction method**, using the ansatz:

$$\mathcal{A}(z) = d\ln(az^2+1) + d\ln(bz^4+1) + mz^2/4 + pz^4/4 + ...$$

$$f(z) = e^{(cz^2+nz+k-A(z)+...)}$$

with free parameters $\{L,\, a,\, b,\, c,\, d,\, k,\, n,\, m,\, p,\, G_5, ...\}$.

Common Themes

- ML used to **reconstruct bulk geometry** from boundary QFT data.
- Goal: reliable **equation of state**, transport coefficients, and **phase structure** of strongly coupled QCD matter.

Holographic Models: Conventional vs. ML

Conventional Holographic model **ML Holographic model**

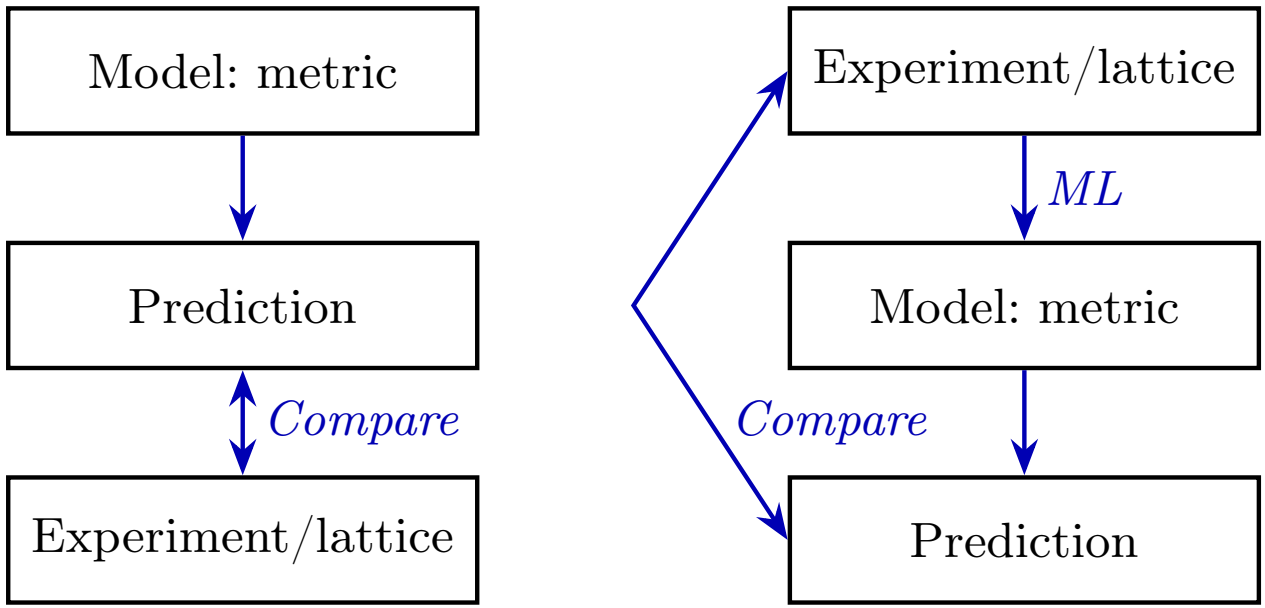

X. Chen and M. Huang, JHEP **02** (2025), 123

Flavor-Dependent CEP Locations in the T–μ_B Plane

	μ_B^c (GeV)	T^c (GeV)
$N_f = 2$	0.46	0.147
$N_f = 2+1$	0.74	0.094
$N_f = 2+1+1$	0.87	0.108

I. Ya. Aref'eva's talk

Conclusion

- String tensions (TWL, SWL) and the JQ parameter are calculated for models incorporating two types of anisotropy. Under variations of thermodynamic parameters — temperature T, chemical potential μ, and magnetic field — the string tensions and JQ parameter undergo phase transitions.

Conclusion

- String tensions (TWL, SWL) and the JQ parameter are calculated for models incorporating two types of anisotropy. Under variations of thermodynamic parameters — temperature T, chemical potential μ, and magnetic field — the string tensions and JQ parameter undergo phase transitions.
- The JQ parameter can serve as an indicator of first-order phase transitions, while the temporal Wilson loop signals the confinement/deconfinement transition, and the SWL reveals an additional phase transition.

Conclusion

- String tensions (TWL, SWL) and the JQ parameter are calculated for models incorporating two types of anisotropy. Under variations of thermodynamic parameters — temperature T, chemical potential μ, and magnetic field — the string tensions and JQ parameter undergo phase transitions.
- The JQ parameter can serve as an indicator of first-order phase transitions, while the temporal Wilson loop signals the confinement/deconfinement transition, and the SWL reveals an additional phase transition.
- Machine learning represents a powerful method for AdS/QCD models. It would therefore be of significant interest to incorporate the behavior of different Wilson loops into a unified framework using machine learning.

Conclusion

- String tensions (TWL, SWL) and the JQ parameter are calculated for models incorporating two types of anisotropy. Under variations of thermodynamic parameters — temperature T, chemical potential μ, and magnetic field — the string tensions and JQ parameter undergo phase transitions.
- The JQ parameter can serve as an indicator of first-order phase transitions, while the temporal Wilson loop signals the confinement/deconfinement transition, and the SWL reveals an additional phase transition.
- Machine learning represents a powerful method for AdS/QCD models. It would therefore be of significant interest to incorporate the behavior of different Wilson loops into a unified framework using machine learning.

What's next?
The following steps involve the selection of training data, accounting for anisotropic effects, and describing diverse datasets within a single realistic model

Conclusion

- String tensions (TWL, SWL) and the JQ parameter are calculated for models incorporating two types of anisotropy. Under variations of thermodynamic parameters — temperature T, chemical potential μ, and magnetic field — the string tensions and JQ parameter undergo phase transitions.
- The JQ parameter can serve as an indicator of first-order phase transitions, while the temporal Wilson loop signals the confinement/deconfinement transition, and the SWL reveals an additional phase transition.
- Machine learning represents a powerful method for AdS/QCD models. It would therefore be of significant interest to incorporate the behavior of different Wilson loops into a unified framework using machine learning.

What's next?
The following steps involve the selection of training data, accounting for anisotropic effects, and describing diverse datasets within a single realistic model

Thank you for your attention!

Backup. Light-like Wilson loops

$$ds^2 = \frac{L^2 e^{2\mathcal{A}_s}}{z^2}\left(-g(z)dt^2 + dx_1^2 + \left(\frac{z}{L}\right)^{2-2/\nu}\left(dx_2^2 + e^{c_B z^2}dx_3^2\right) + \frac{dz^2}{g(z)}\right)$$

$$dt = \frac{dx_+ + dx_-}{\sqrt{2}},\ dx_1 = \frac{dx_+ - dx_-}{\sqrt{2}}.$$

The contour $\mathcal{C}$: "short sides" with length ℓ along the x_3(or x_2) direction and the "long sides" with length L_- along the x_- direction

$$x_- = \tau; \qquad x_3(or\, x_2) = \xi$$

$$S_{NG,3} = \frac{L^2 L_-}{\pi\alpha'}\int_0^{\frac{\ell}{2}} d\xi\, \frac{e^{2A_s(z)}}{z^2}\sqrt{\frac{1-g(z)}{2}\left(e^{c_B z^2}\left(\frac{z}{L}\right)^{2-2/\nu} + \frac{z'^2}{g(z)}\right)}$$

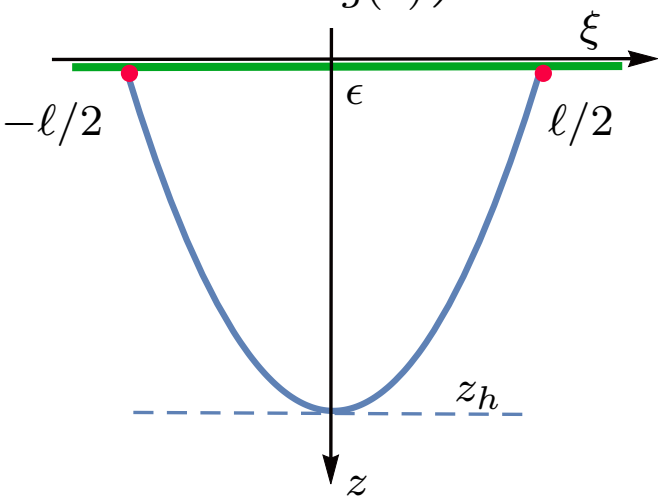

The integral of motion

$$P = \frac{e^{2A_s(z)}(g(z)-1)}{\sqrt{2}z^2 g(z)\sqrt{(1-g(z))\left(e^{c_B z^2}\left(\frac{z}{L}\right)^{2-\frac{2}{\nu}} + \frac{z'^2}{g(z)}\right)}}$$

and we get for z'

$$z' = \frac{e^{2A_s + c_B z^2\left(\frac{z}{L}\right)^{-2/\nu}}}{\sqrt{2}L^2 P}\sqrt{g(1-g) - 2gL^2P^2z^2\left(\frac{z}{L}\right)^{2/\nu}e^{-4A_s - c_B z^2}}$$

Light-like Wilson loops

"Returning point":

$$g(z_*)\underbrace{\left((1-g(z_*))e^{4A_s+c_B z_*^2}-2L^2P^2z_*^2\left(\frac{z_*}{L}\right)^{2/\nu}\right)}_{\mathcal{I}}=0 \quad (*)$$

Equation (*) has two possible solutions:

$$\begin{aligned} &a) \quad g(z_*)=0, \quad \text{this hold for} \quad z_*=z_h, \\ &b) \quad \mathcal{I}=0, \text{in our case is unstable} \end{aligned}$$

- **a)** $z_*=z_h$.

$$\begin{aligned} \frac{\ell}{2} &= PL^2\int_0^{z_h}\frac{\sqrt{2}e^{-2\mathcal{A}_s-c_Bz^2}\left(\frac{z}{L}\right)^{2/\nu}}{\sqrt{g(1-g)}}dz+\ldots \\ \frac{\mathcal{S}}{2} &= S_0+L^2P^2\int_0^{z_h}\frac{e^{-2\mathcal{A}_s(z)-c_Bz^2}\left(\frac{z}{L}\right)^{2/\nu}dz}{\sqrt{2g(1-g)}}+\ldots \end{aligned}$$

I. Y. Aref'eva, A. Hajilou, A. Nikolaev and P. S., PRD **112** (2025) 126007

Arbitrary orientation for JQ

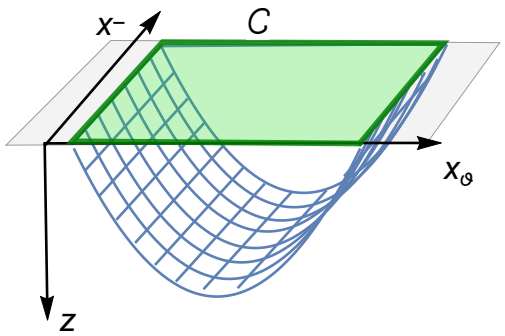

$$ds^2 = \frac{L^2 \mathfrak{b}_s(z)}{z^2}\left[-g(z)dt^2 + \mathfrak{g}_1 dx^2 + \mathfrak{g}_2 dy_1^2 + \mathfrak{g}_3 dy_2^2 + \frac{dz^2}{g(z)}\right],$$

$$\hat{q} = \frac{L^2}{\pi\alpha' a}, \qquad a = \frac{L^2 L^-}{2\sqrt{2}\pi\alpha'}\int_0^{z_h}\frac{dz}{\mathcal{F}(z)M(z)}.$$

$$x^- = \tau, \qquad x_j = \xi\sin\theta, \qquad x_k = \xi\cos\theta, \qquad x^+ = const, \qquad z = z(\xi),$$

$$i, j, k \quad \text{are distinct and} \quad i, j, k = 1, 2, 3$$

$$a_\theta = \int_0^{z_h}\frac{z^2 dz}{(\mathfrak{g}_j(z)sin^2\theta + \mathfrak{g}_k(z)cos^2\theta)\mathfrak{b}_s(z)\sqrt{(\mathfrak{g}_i(z) - g(z))g(z)}}$$

P.S., Mosc. Univ. Phys. Bull.'25

Spatial Wilson loops. Parametrization

To describe the nesting of the 2-dimensional world sheet in 5-dimensional spacetime we use

$$\begin{aligned} X^0(\xi) &= const, \\ X^i(\xi) &= \sum_{\alpha=1,2} a_{i\alpha}(\phi,\theta,\psi)\,\xi^\alpha, \qquad i=1,2,3, \\ X^4(\xi) &= z(\xi^1), \end{aligned}$$

x^i are spatial coordinates and $a_{ij}(\phi,\theta,\psi)$ are entries of the rotation matrix. Here ϕ is the angle between ζ^1-axis and the node line (N), θ is the angle between ζ^3 and x^3-axes, ψ is the angle between the node line N and x^1-axis.

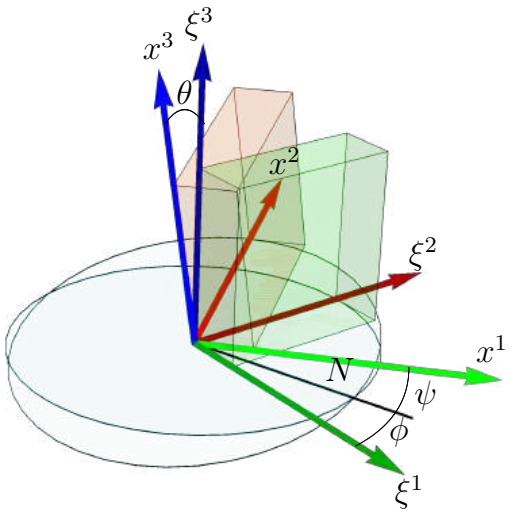

$$\begin{aligned} a_{11}(\phi,\theta,\psi) &= \cos\phi\cos\psi - \cos\theta\sin\phi\sin\psi, \\ a_{12}(\phi,\theta,\psi) &= -\cos\psi\sin\phi - \cos\phi\cos\theta\sin\psi, \\ a_{13}(\phi,\theta,\psi) &= \sin\theta\sin\psi, \\ a_{21}(\phi,\theta,\psi) &= \cos\theta\cos\psi\sin\phi + \cos\phi\sin\psi, \\ a_{22}(\phi,\theta,\psi) &= \cos\phi\cos\theta\cos\psi - \sin\phi\sin\psi, \\ a_{23}(\phi,\theta,\psi) &= -\cos\psi\sin\theta, \\ a_{31}(\phi,\theta,\psi) &= \sin\phi\sin\theta, \\ a_{32}(\phi,\theta,\psi) &= \cos\phi\sin\theta. \\ a_{33}(\phi,\theta,\psi) &= \cos\theta. \end{aligned}$$

Nambu-Goto action for Spatial Wilson Loop

Spatial Wilson loop (SWL):

$$\mathcal{S}_{SWL} = \int_{\mathcal{W}} \left(\frac{L^2 b_s}{z^2}\right) \sqrt{\left(\mathfrak{g}_1\mathfrak{g}_2 a_{33}^2 + \mathfrak{g}_1\mathfrak{g}_3 a_{23}^2 + \mathfrak{g}_2\mathfrak{g}_3 a_{13}^2 + \frac{z'^2}{g}\,\bar{g}_{22}\right)}\, d\xi^1 d\xi^2$$

$$\mathcal{V}_{SWL}(z) = \left(\frac{L^2 b_s}{z^2}\right) \sqrt{\mathfrak{g}_1\mathfrak{g}_2 a_{33}^2 + \mathfrak{g}_1\mathfrak{g}_3 a_{23}^2 + \mathfrak{g}_2\mathfrak{g}_3 a_{13}^2}$$

Holographic entanglement entropy (HEE):

$$\mathcal{S}_{HEE} = \int_{\mathcal{P}} \left(\frac{L^2 b_s}{z^2}\right)^{3/2} \sqrt{\left(\mathfrak{g}_1\mathfrak{g}_2\mathfrak{g}_3 + \frac{z'^2}{g}\,(\bar{g}_{22}\bar{g}_{33} - \bar{g}_{23}^2)\right)}\, d\xi^1 d\xi^2 d\xi^3,$$

$$\mathcal{V}_{HEE}(z) = \left(\frac{L^2 b_s}{z^2}\right)^{3/2} \sqrt{\mathfrak{g}_1\mathfrak{g}_2\mathfrak{g}_3},$$

g, $\mathfrak{g}_1$, $\mathfrak{g}_2$, $\mathfrak{g}_3$ are functions of z and $\bar{g}_{22}$, $\bar{g}_{33}$, $\bar{g}_{23}$ are functions of z and the Euler angles:

$$\begin{aligned}
\bar{g}_{22}(z,\phi,\theta,\psi) &= \mathfrak{g}_1 a_{12}^2 + \mathfrak{g}_2 a_{22}^2 + \mathfrak{g}_3 a_{32}^2,\\
\bar{g}_{33}(z,\phi,\theta,\psi) &= \mathfrak{g}_1 a_{13}^2 + \mathfrak{g}_2 a_{23}^2 + \mathfrak{g}_3 a_{33}^2,\\
\bar{g}_{23}(z,\phi,\theta,\psi) &= \mathfrak{g}_1 a_{12} a_{13} + \mathfrak{g}_2 a_{22} a_{23} + \mathfrak{g}_3 a_{32} a_{33}
\end{aligned}$$

I. Y. Aref'eva, A. Patrushev, P.S. JHEP **07**, 043 (2020)

Born-Infeld type action (1-dim dynamic model):

$$\mathcal{S} = \int_{-\ell/2}^{\ell/2} M(z(\xi))\sqrt{\mathcal{F}(z(\xi)) + (z'(\xi))^2}\, d\xi, \quad V(z(\xi)) = M(z(\xi))\sqrt{\mathcal{F}(z(\xi))}$$

We have two options to have $\ell \to \infty$ I. Aref'eva, EPJ Web Conf. **191**, 05010 (2018)

Born-Infeld type action. First option.

1) The existence of a stationary point of $\mathcal{V}(z)$ for $0 < z < z_h$: $\mathcal{V}'\Big|_{z_{DW}} = 0$.

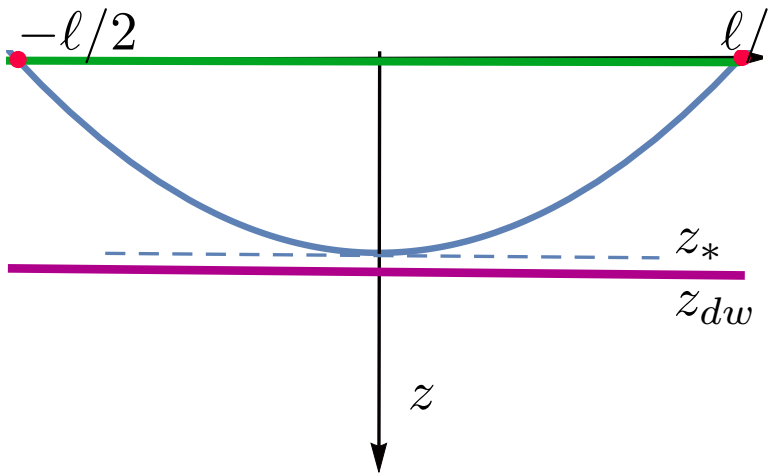

$$\ell \underset{z\to z_{DW}}{\sim} \frac{1}{\sqrt{F(z_{DW})}} \sqrt{\frac{\mathcal{V}(z_{DW})}{\mathcal{V}''(z_{DW})}}\, \log(z - z_{DW}),$$

$$\mathcal{S} \underset{z\to z_{DW}}{\sim} M(z_{DW}) \sqrt{\frac{\mathcal{V}(z_{DW})}{\mathcal{V}''(z_{DW})}}\, \log(z - z_{DW}).$$

$$\mathcal{S} \quad \sim \quad \sigma_{DW} \cdot \ell,$$

$$\sigma_{DW} \quad = \quad M(z_{DW}) \sqrt{F(z_{DW})}.$$

Born-Infeld type action. Second option.

2) There is no stationary point of $\mathcal{V}(z)$ in the region $0 < z < z_h$ and we suppose it to be near horizon

$$F(z) = \mathfrak{F}(z_h)(z_h - z) + \mathcal{O}((z_h - z)^2),$$

if $M(z) \underset{z \to z_h}{\to} \infty$ as

$$M(z) \underset{z \sim z_h}{\sim} \frac{\mathcal{M}(z_h)}{\sqrt{z - z_h}},$$

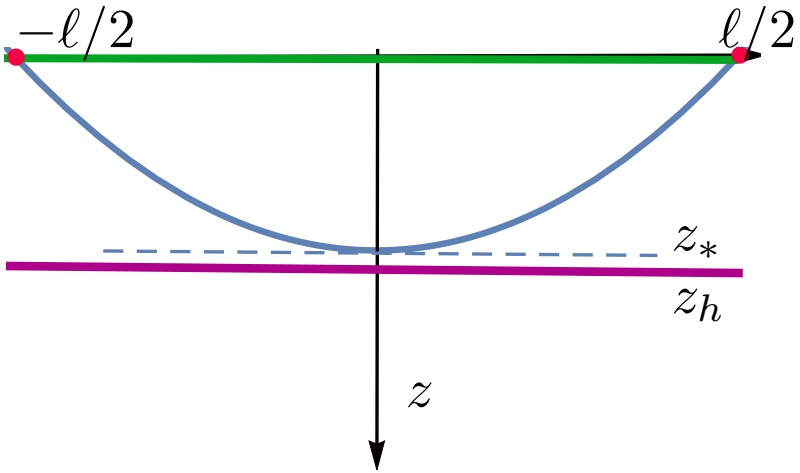

$$\ell \underset{z \to z_h}{\sim} \frac{1}{\sqrt{\mathfrak{F}(z_h)}} \frac{1}{\sqrt{-\frac{2\mathcal{V}'(z_h)}{\mathcal{V}(z_h)}}} \log(z - z_h),$$

$$\mathcal{S} \underset{z \to z_h}{\sim} \mathcal{M}(z_h) \frac{1}{\sqrt{-\frac{2\mathcal{V}'(z_h)}{\mathcal{V}(z_h)}}} \log(z - z_h).$$

$$\sigma_h = \mathcal{M}(z_h) \sqrt{\mathfrak{F}(z_h)} = M(z_h) \sqrt{F(z_h)}.$$

DW equations for SWLs

The equations for the DW for SWL in particular cases for different orientations:

$$xY_1 \text{ and } Xy_1: \quad \left.\frac{2b_s'(z)}{b_s(z)}+\frac{\mathfrak{g}_1'(z)}{\mathfrak{g}_1(z)}+\frac{\mathfrak{g}_2'(z)}{\mathfrak{g}_2(z)}-\frac{4}{z}\right|_{z=z_{DW}}=0,$$

$$xY_2: \quad \left.\frac{2b_s'(z)}{b_s(z)}+\frac{\mathfrak{g}_1'(z)}{\mathfrak{g}_1(z)}+\frac{\mathfrak{g}_3'(z)}{\mathfrak{g}_3(z)}-\frac{4}{z}\right|_{z=z_{DW}}=0,$$

$$y_1Y_2: \quad \left.\frac{2b_s'(z)}{b_s(z)}+\frac{\mathfrak{g}_2'(z)}{\mathfrak{g}_2(z)}+\frac{\mathfrak{g}_3'(z)}{\mathfrak{g}_3(z)}-\frac{4}{z}\right|_{z=z_{DW}}=0.$$

I Aref'eva, K. Rannu, P.S., TMPh, 206:3 (2021) [arXiv:2012.05758]